*Revision, changes marked
Click here to view linked References

SO_2 flux and the thermal power of volcanic eruptions

Richard W. Henley[1,*] and Graham O. Hughes[2]

1. Research School of Earth Sciences, Australian National University, Canberra, ACT, Australia

2. Department of Civil and Environmental Engineering, Imperial College, London, England

* Corresponding author: r.143.henley@gmail.com

Abstract

A description of the dynamics, chemistry and energetics governing a volcanic system can be greatly simplified if the expansion of magmatic gas can be assumed to be adiabatic as it rises towards the surface. The conditions under which this assumption is valid are clarified by analysis of the transfer of thermal energy into the low conductivity wallrocks traversed by fractures and vents from a gas phase expanding over a range of mass flux rates. Adiabatic behavior is predicted to be approached typically within a month after perturbations in the release of source gas have stabilized, this timescale being dependent upon only the characteristic length scale on which the host rock is fractured and the thermal diffusivity of the rock. This analysis then enables the thermal energy transport due to gas release from volcanoes to be evaluated using observations of SO_2 flux with reference values for the H_2O:SO_2 ratio of volcanic gas mixtures discharging through high temperature fumaroles in arc and mantle-related volcanic systems. Thermal power (MW_H/s) estimates for gas discharge are $10^{1.8}$ to $10^{4.1}$ MW_H during quiescent, continuous degassing of arc volcanoes and $10^{3.7}$ to $10^{7.3}MW_H$ for their eruptive stages, the higher value being the Plinean Pinatubo eruption in 1991. Fewer data are available for quiescent stage mantle-related volcanoes (Kilauea $10^{2.1}MW_H$) but for eruptive events power estimates range from $10^{2.8}$ MW_H to $10^{5.5}MW_H$. These estimates of thermal power and mass of gas discharges are commensurate with power estimates based on the total mass of gas ejected during eruptions. The sustained discharge of volcanic gas during quiescent and short-lived eruptive stages can be related to the hydrodynamic structure of volcanic systems with large scale gaseous mass transfer from deep in the crust coupled with episodes of high level intrusive activity and gas release.

Key words

Volcanic magmatic gas adiabatic expansion power

1. Introduction

Much of what we know about fluid processes inside degassing volcanic systems is inferred from surface observations of quite shallow thermal features such as fumaroles, solfatara and volcanic lakes. Volcanic hazard risk management primarily depends on estimates of the rates of change of these phenomena in conjunction with seismic monitoring. However our fundamental understanding of the physics of volcanoes and their eruptive histories still suffers from the lack of quantification of the energetics of these processes. Post facto estimates of the mass of erupted material as lavas or dispersed ash provide some idea of the scales of eruptive activity (Pyle, 2015) but not of the substantial thermal energy transport between and during eruptions through discharge of volcanic gas.

The advent of remote sensing methods for monitoring SO_2 gas flux into the atmosphere now provides information that allows quantification of the scale of subsurface heat and mass transfer through active volcanoes. In this paper we show how these data in combination with reference volcanic gas compositions may be used to estimate the thermal energy transport inside degassing volcanoes and to provide a comparative scale of the relative magnitudes of thermal energy release from quiescent and erupting volcanoes. In order to achieve this we first need to consider how much thermal energy is lost to the rock mass that makes up a volcanic system as magmatic gas expands and flows through to the surface. This heat transfer problem may be reframed as a model for quantifying the time that is required for a volcanic system to regain a steady thermal state following perturbation with respect to heat transfer to and from the rock medium

2. Heat and Mass Transfer in active volcanoes

Volcanic systems are loci of sustained heat and mass transfer through the Earth's crust (Elder, 1965). Understanding of the basic physics and chemistry that control their behaviour through time is obtained through application of thermodynamic principles within the context of some crucial underlying assumptions. One of these is that magmatic gas expansion through the fractured host rocks beneath volcanoes may be considered *adiabatic* (in this context the term 'adiabatic' means that heat transfer from an expanding magmatic gas to and from the rock mass is zero[1]). However it is axiomatic that, whenever a temperature gradient occurs between gas and rock, *some* heat is transferred by conduction across fracture boundaries into the low conductivity host rocks where a thermal buffer develops. The thermal buffer then limits the proportion of heat lost from the gas flow to the rock mass so that its magnitude (relative to the heat flux of expanding magmatic gas and the transfer of heat on a range of time and length scales within the host rock) underlies the reasonableness of assumptions of *adiabatic expansion* of magmatic gas mixtures. In practical terms the system, following perturbation adjusts to a minimal heat transfer condition that *approximates* an adiabatic state.

[1] In this limit the surface temperature of the host rock matches that of the gas (where they are in thermal contact) and the temperature gradient in the rock in a direction locally normal to its surface is zero. Although a gradual decrease of temperature towards the surface must exist in the host rock network as the background pressure decreases, heat loss due to conduction away from the expanding gas flow through the rock (which corresponds to a loss of thermal energy from the gas in order to maintain the temperature field in the rock) can be assumed negligible in comparison to the magnitude of the heat flux carried by the gas.

2.1 Heat transfer between expanding magmatic gas and a fractured rock mass

Here we proceed to characterise the proportion of heat that, as a function of time and the properties of the rock mass, is transferred conductively into the rock mass from an expanding magmatic gas mixture. We adopt a fractured block model (Figure 1, inset) wherein gas expansion occurs through the 'cracks' between blocks of rock of characteristic dimension (*d*) with transfers of thermal energy through a thermal boundary layer in the low conductivity rock medium (Henley and Hughes, 2000). We consider the process of adjustment from one thermally-equilibrated state to another following a sudden perturbation at time $t = 0$ in the magmatic gas source. The adjustment dynamics governing subsurface expansion of the gas may also have relevance to a time-varying source, and we comment on this towards the end of this paper. For convenience we here use the term *magmatic gas ('magma-related')* to refer to gas mixtures expanding through the superstructure of volcanic systems and derived from intrusive complexes and other deep sources (Shinohara, 2013) and *volcanic gas* for the gas mixtures discharged to the atmosphere during quiescence through vents and high temperature fumaroles and with particulates the gas mixtures discharged during eruptions.

A perturbation in the magmatic gas source, such as increased permeability due to rock stress release or intrusion (Tibaldi, 2015) will first lead to a broad-scale adjustment in gas temperature and pressure along flow paths in the host rock through which it expands. The time scale, t_1, on which this occurs is assumed *a priori* to be a) sufficiently rapid compared with the other adjustment processes, and b) consistent with supposing that gas is able to percolate through the fracture network in the host rock relatively freely given its lower resistance to flow and the absence of wettability effects associated with liquid–solid contact. An estimate of this time scale may be made using Darcy's law,

$$t_1 \sim \frac{h\phi\mu}{K dp/dz}, \qquad (1)$$

where h is the height through which the gas rises, K and ϕ are the characteristic permeability and porosity of the host rock, respectively, μ is the dynamic viscosity of the gas and dp/dz is the broad-scale vertical pressure gradient driving the rise of gas. As we will see t_1 is typically on the order of days.

Following the initial perturbation, the temperature field in the host rock starts adjusting towards thermal equilibrium; transient behaviour is expected in the surface discharge. At some time, which we denote as $t = t_2$, the temperature field in the rock no longer evolves significantly in the time taken for a gas parcel to rise to the surface; the surface discharge might be expected to stabilise, but continue to evolve at a more gradual rate. Beyond this time, we might anticipate the possibility of a quasi-adiabatic state (at $t = t_3$), in which the process of gas expansion involves a relatively small amount of heat exchange with the host rock (and the surface discharge is expected to be quasi-steady). Eventually, at large times, the full adiabatic steady state (described earlier) and thermal equilibrium will be attained.

We now proceed to make rough estimates of the above time scales and the volume of host rock (which we refer to as the thermal buffer region) involved in the adjustment process. We assume that the adjustment process is longer than the time t_1 required to establish the gas pressure and temperature field that forces percolation through the fracture network in the host rock. Specifically,

we assume that the thermal inertia of the rock component blocks in the network governs the response of the buffer region.

Within each block, the evolution of the temperature field T may be described by the diffusion equation in the form:

$$\rho_r c_p \frac{\partial T}{\partial t} = k\nabla^2 T \,, \qquad (2)$$

where k, ρ_r and c_p are the thermal conductivity, density and specific heat capacity of the rock, respectively, and t is time. We now manipulate this equation to obtain scales for the quantities of interest. A thermal boundary layer of thickness $\delta(t)$ grows in time by conduction in the rock, accommodating the change in external temperature, wherever the block surface is exposed to the magmatic gas:

$$\delta \sim (\kappa t)^{1/2} \,, \qquad (3)$$

where $\kappa = k/\rho_r c_p$ is the thermal diffusivity of the rock (Henley and Hughes, 2000).

We may use equation 3 to estimate t_2 as the time at which $\Delta\delta/\delta(t_2) = c << 1$, where $\Delta\delta$ is the change in boundary layer thickness during the transit time of a gas parcel t_1 and c is a suitably small threshold value, e.g. 10%. Thus we find that $t_2 = t_1/c$ (>> t_1).

If A_r is the total surface area of rock in the fracture network, we can write equation 3 in the form: (by integrating over the volume $A_r\delta$ and applying the Divergence Theorem):

$$\frac{\partial}{\partial t}\left(\rho_r c_p A_r \delta T\right) = \rho_r c_p A_r \delta \frac{\partial T}{\partial t} + \rho_r c_p A_r T \frac{\partial \delta}{\partial t} = k A_r \nabla T_s, \qquad (4)$$

where the first term on the far left represents the rate of change of thermal energy stored in the host rock (which can be split into the sum of two terms shown – the first representing the contribution owing to an evolving temperature in the boundary layer and the second representing the contribution from a evolving boundary layer thickness). The subscript s in equation 4 denotes the solid surface in thermal contact with the gas. A straightforward order of magnitude estimate (using equation 3) suggests that all terms in equation 4 are of the same order, i.e.

$$\frac{\partial}{\partial t}\left(\rho_r c_p A_r \delta T\right) \sim \rho_r c_p A_r \delta \frac{\partial T}{\partial t} \sim \rho_r c_p A_r T \frac{\partial \delta}{\partial t} \sim k A_r \nabla T_s \sim O\left(\rho_r c_p A_r \Delta T \kappa^{1/2} t^{-1/2}\right) \qquad (5)$$

where the temperature change at $t = 0$ is ΔT. Note that equations 3-5 implicitly assume the growing thermal boundary layers do not interact, but this becomes invalid when δ is of the same order as the block size (from equation 3, this occurs when $t \sim d^2/\kappa$). In this regime the temperature contrast in the block is not maintained at ΔT and reduces towards zero. Thus the host rock approaches thermal equilibrium and cannot store (or reject) any more heat. Hence, for the passage of magmatic gas to be approximately adiabatic, we require that either the rate of heat transfer from the gas (the last term in equation 4) be much less than the energy flux E through the system (termed the quasi-adiabatic regime) or the thermal boundary layer thickness to have become comparable to the block size, leading to fully adiabatic behaviour. To estimate the time t_3 at which this occurs, we estimate the surface area A_r of rock in the fracture network by simply assuming that the host rock volume ($A_s h$) is fractured into regular cubical blocks with dimension d so that

$$A_r = \frac{6A_s h}{d}. \qquad (6)$$

Field data show that the effective block size or fracture spacing of volcanic systems is much smaller than d = 1 m. For example at Ruapehu, New Zealand, Massiot et al. (2014) measured a median spacing of 0.36 m. and La Felice et al.(2014) measured spacings of 0.15 to 0.25m to 520m depth at Mt Amiata, Italy. Heap et al. (2015) showed that permeabilities of 10^{-12}m^2 were attributable to both macrofractures and high density networks of microfractures in andesite at Colima, Mexico. Moreover Hautmann et al. (2014) showed using strain field analysis that high permeability was sustained at Soufrière Hills, by networks of fractures that were maintained by hydraulic fracturing due to gas pressure.

We proceed to approximate the host rock volume as a cylinder, where A_s is the cross-sectional area observable at the surface. This approach is expected to lead to a generous estimate of A_r using equation 6 because the actual cross-sectional area of host rock is likely to be smaller than A_s at depth. Using equations 4 and 5, behaviour that is either quasi-adiabatic (i.e. $kA_r\nabla T_s \ll E$) or fully adiabatic (i.e. $\delta >> d$) is anticipated for the sooner of

$$t_3' \gg \left(\frac{6\rho_r c_p \Delta T A_s h}{E}\right)^2 \frac{\kappa}{d^2} \qquad (7a)$$

or,

$$t_3'' \gg \frac{d^2}{\kappa}. \qquad (7b)$$

From the two conditions in equation 7, we therefore expect to see the appearance of a quasi-steady adiabatic gas expansion regime only if $t_3' < t_3''$, which requires

$$d \geq D \qquad (8)$$

where $D = \left(\frac{6\rho_r c_p \Delta T A_s h\kappa}{E}\right)^{1/2}$ is a threshold block size.

In physical terms, a quasi-adiabatic state will be observed only if the block size d is large enough that the thermal boundary layers growing towards the interior of the block do not interact *and* the rate at which thermal energy is transferred from the gas to the host rock has become small compared with the energy flux E through the system. For values of d less than the threshold block size D the host rock blocks will reach full thermal equilibrium first.

2.2 Time scale estimates for the initial response phases

We may now base quantitative estimates for the time scales t_1 and t_2 on observable surface properties and typical properties of rock and water as a gas phase. The permeability K of volcanic rocks range from very low (10^{-16} m^2) to very high (10^{-8} m^2); for unconsolidated rocks with strong connectivity of pore space (i.e. fractures), K can be of order 10^{-10} m^2 (Collinson and Neuberg, 2012). Basing an estimate for t_1 on a conservative value for K = 10^{-12} m^2, with a porosity ϕ in the range 1-10%, a dynamic viscosity for the gas of μ = 30 x 10^{-6} Pa, and a vertical pressure difference of 120 MPa over a rise height h = 4000 m, we predict t_1 can be up to several days (Figure 1). Thus we expect the temperature field in the thermal boundary layers of the host rock blocks to become quasi-steady (as far as the effect on an individual gas parcel is concerned) on time scales t_2 of less than a month. At

this time processes may be reasonably modelled as adiabatic. On shorter time scales the adiabatic assumption cannot reliably be used in thermal or chemical modelling of magmatic gas expansion through volcanic systems.

2.3 Quasi-adiabatic and adiabatic behaviour

2.3.1 Thermal power of volcanic discharges

The heat transfer analysis provided here for magmatic gas expanding through the fractured rock mass beneath volcanoes indicates below that thermal equilibration is achieved with respect to fractured rocks on a time scale of 10 days to 3 years for block sizes between 1 and 10m. As we have seen in §2.2, the initial broad scale adjustment of gas pressure and temperature through the network of fractures between blocks is likely to be significantly shorter and on the scale of a few days. Since gas discharge from quiescent volcanoes occurs over a much longer time scale it may be regarded as occurring in a quasi-steady state such that expansion flow paths may be considered as adiabatic. Any actual expansion path (in pressure–temperature-enthalpy-entropy space) at any time is likely to be stepped due to successive throttles within a continuously evolving fracture array within the volcano.

Further assessment of thermal equilibration timescales (such as estimates of t_3') of the gas expansion process beyond $t \sim t_2$ requires specific data regarding the associated energy and mass transport. Mass transfer estimates have only become available recently through remote sensing of SO_2 fluxes ($\Theta_{S_{tg}}$) for a number of quiescent but continuously degassing volcanoes (Supplement 1). Since volcanic gas mixtures are dominated by water (> 90 mole percent in arc volcanic gases – see Supplement 2) the total mass flux (Θ_G) due to gas release and the heat flux ($\Sigma H'_G$) of a volcano may then be estimated by using the mole fraction of SO_2, x_{SO_2}, in the discharge (Matsushima et al., 2003) through,

$$\Theta_G = 1/x_{SO_2}.\Theta_{S_{tg}} \qquad (9a)$$

$$\Sigma H'_G = H'_G.\ \Theta_G \qquad (9b)$$

where and H'_G is the enthalpy of the gas mixture which, for salt contents of less than about 10 weight percent, may be taken as that of water. Application of these equations to individual volcanoes depends upon translation of SO_2 flux data into total mass flux due to gas release into volcanic plumes. In turn this requires an estimate of the ratio of H_2O to SO_2 in the gas plume but remote sensing estimates for H_2O flux are far more difficult to achieve. In order then to provide relative thermal power estimates for the quiescent, continuously degassing through eruptive stages of volcanic activity it is convenient to use reference values derived from sampling of high temperature fumaroles.

2.3.2 Reference volcanic gas compositions

The compositions of volcanic gas mixtures are obtained through meticulous sampling in extreme environments (de Moor et al., 2013; Fischer, 2008; Giggenbach and Matsuo, 1991; Giggenbach et al., 2001; Shinohara, 2013; Zelenski and Taran, 2011). Supplement 1 provides a compilation of 70 published analyses of volcanic gases from fumaroles at temperatures greater than 500 °C for the

molar concentrations of the major gases within volcanic gas mixtures released into the sub-structure of volcanoes from mid and upper crustal intrusive complexes and other sources. For convenience they are broadly subdivided into arc and mantle-related provenances. The latter are few since most mantle-sourced volcanism occurs on the sea floor so that direct gas sampling is not possible. H_2O (> ~ 80 mole percent), CO_2 and S, as a range of gas phase sulphur species , are the principle components of these mixtures. HCl, HF and H_2 are also major components at lower concentration. Minor components include metastable species that may have transient existence in these reactive environments, and unreactive nitrogen and noble gases that are important traces of source interactions for volcanoes (Sano and Fischer, 2013).

A range of factors such as accessibility determine that the fumarole gas data are a non-random sampling of all active volcanic systems. In order to derive reference values for $\underline{x}_{St}$ and $\underline{H}'_G$, we have therefore calculated median values of these data (Table 2) since medians are a more reliable measure than means for the small and highly skewed sample population in this data set. We also applied a temperature filter of 800-1000°C in order to remove possible dilution and condensation effects that may occur in the high level superstructure of volcanoes and during sampling (Botcharnikov et al., 2003; Giggenbach and Matsuo, 1991; Giggenbach and Sheppard, 1989; Giggenbach et al., 2001). This filter removed some outlier values such as the water-rich 1100 °C data from Klyuchevskoi volcano, Kamchatka. Expressed as mole percent (100 x mole fraction) the median (n=24) of the high temperature (800-1000°C) data for arc volcanoes is as follows, 870°C, H_2O= 95.0, CO_2 = 1.6, S_t = 1.8 (fifty percent of the values of x_{St} lie within a factor of two of this median value), HCl = 0.5, HF=0.04, H_2 = 0.8 mole percent $\underline{x}_{St}$ = 52.8; a slightly lower value ($\underline{x}_{St}$ = 52.1) is obtained by filtering out the water-rich fumarole analysis from Showashinzan volcano, Japan (Mizutani and Sugiura, 1982). As has been observed elsewhere (Carmichael et al., 1974; Giggenbach, 1996; Symonds et al., 1994; Verhoogen, 1949; Williams and McBirney, 1979), high temperature arc gases are significantly more water-rich and lower in CO_2 than mantle-derived basaltic gases. CO_2, and sulfur species (SO_2 > H_2S) are the most abundant component relative to the other major gases.

Analytical values of x_{S_t} do not directly provide values of x_{SO_2} since disproportionation of SO_2 to H_2S and other reduced sulfur species occurs during the temperature decrease that results from the adiabatic expansion of magmatic gas mixtures from their sub-volcanic source regimes as well as through heterogeneous gas-mineral reactions (Henley et al., 2015). Figure 2 shows the variation of molar concentrations (For a given component, *i*, mole percent$_i$ = 100 x x_i) for sulfur species at 1 bar total pressure as a function of temperature. The dominance of SO_2 above about 800 °C is clear such that for fumaroles sampled above this temperature it is reasonable to assume that $x_{SO_2} = x_{S_t}$.

2.3.3 Thermal magnitudes of erupting volcanoes

In the absence of alternative direct methods, it is permissible as well as practical to use the reference values of total sulfur concentration ($\underline{x}_{S_t}$) as proxies for x_{SO_2} in the application of equation 9a to obtain comparative estimates of the thermal magnitudes of volcanic gas discharges (Figure 3 and Supplement 3). At its median temperature of 870 °C the reference arc volcanic gas mixture has an estimated enthalpy ($\underline{H}'_G$), of about 4300 kJ/kg at 1 bar total pressure (100 kPa) and $\underline{x}_{St}$ of 0.013, equivalent to a H_2O/SO_2 *mass ratio* of 21. Using this reference value, Table 2 shows that the total gas fluxes (~ 95 mole percent H_2O) from individual continuously degassing arc volcanoes range from 1 to 85 megatonnes per day with heat fluxes from $10^{1.8}$ to $10^{3.6}$ MW_H. Etna has a wide range during

continuous degassing ($10^{3.6}$ to $10^{4.4}$ MW_H) . Kilauea, as a representative of mantle-sourced gas discharge, has a thermal power estimate of 900 tonnes SO_2 per day, which at $10^{2.1}$ MW_H, is in the lower part of this range. By comparison, Erta Ale (Ethiopia) at 100 tonnes SO_2 per day (de Moor et al., 2013), is significantly lower ($10^{1.2}$ MW_H)[2].

The heat fluxes estimated here from SO_2 flux data range from about 100 to 3500 MW_H ($10^{2\text{-}4.4}$ MW_H). For comparison the Wairakei geothermal system (Taupo Volcanic Zone, New Zealand) in its undisturbed state prior to exploitation had a heat flow of about 400 MW_H($10^{2.6}$ MW_H) (Fisher, 1964). Geothermal heat and mass transfer is a consequence of conductive heating into the base of the hydrostatic groundwater regime *and* capture of low fluxes of magmatic gas by quenching into the groundwater flow (Hurwitz et al., 2003). In volcanoes in regions of high rainfall, such as the Cascade volcanoes in western North America, SO_2 discharge may be reduced to zero by dissolution into high level groundwater flows(Symonds et al., 2001).

If the thermal energy of the gas mixture expanding into a volcanic system changes by 10%, equation 7a may be used to estimate the length of time $t = t'_3$ after which we would expect the rate of thermal energy exchanged with the host rock to become much less than the surface heat flux (i.e. the quasi-adiabatic regime). We first base reasonable dimensions for the central core of a quiescent volcano on observable diameters[3] at the surface of 1000 m. Then, taking values for rock of $\kappa \sim 10^{-6}$ m^2/s, ρ_r = 2600 kg/m^3 and c_p = 800 J/kg/K (i.e. k = 2 W/mK (Bonafede and Mazzanti, 1997)), we find (Figure 3b) that for block sizes d [4] between 1 and 50 m, the host rock is predicted to reach thermal equilibrium before a quasi-adiabatic state can be set up, i.e. equation 8 is generally not satisfied in the practical examples considered here. This simplifies the calculations and conclusions considerably; it is important to note that the predicted adjustment is determined by the length scale characterising the fracture network and the thermal diffusivity of the rock, and is independent of any parameters of the volcanic system itself. The timescale t_3'' is predicted to range from about 10 days to 3 years for block sizes between 1 and 10 m, and up to 80 years for block sizes of 50 m. Thus, the gas expansion process will in essence be fully adiabatic after approximately a month to 10 years (i.e. corresponding to complete thermal equilibration of the entire volcanic structure after a few conductive timescales, t_3'', have elapsed), for blocks up to 10 m in size. It is worth further noting that these calculations provide *a posteriori* justification for the assumption that expansion of gas through

[2] Table 2 (and the Supplement 1 table of SO_2 flux data) and estimated power are not provided as a comprehensive review of all the available and continually expanded SO_2 data for active volcanoes. Moreover, for individual volcanoes the temperature and H_2O/SO_2 data used for estimating discharge power may, and should where possible, be specific to that volcano.

[3] We can demonstrate self-consistency of the assumed radial extent with that expected from Darcy's law. We expect that the core radius R expands in the radial direction r such that $dR/dt \sim (K/\phi\mu)\,\partial p/\partial r$. During the rise time ($t_1$; equation 4) of a gas parcel, we therefore expect the core radius at the surface to have increased by an amount $\Delta R_S \sim h(\Delta p_r/\Delta p_z)^{1/2}$, where Δp_r and Δp_z are the typical broad-scale pressure drops in the radial and vertical directions, respectively. With Δp_r ~ 0.5 MPa (an "average" overpressure, which is limited by the fracture strength of the host rock ~ 1 MPa) and Δp_z ~ 120 MPa (the difference in pressure between the surface and a depth of h ~ 4 km), we predict ΔR_s ~ O(250 m).

[4] This range is consistent with the length scale that would be expected based on the fracture strength of the rock (~ 1 MPa, as above) and the broad-scale vertical pressure gradient (~ 0.03 Pa/m). We reason that the local pressure in the rising gas phase can only increase above the prevailing background pressure in the host rock by approximately the fracture strength (before a new fracture is initiated). This criteria suggests d ~ 30 m.

the fracture network inside a volcanic system is relatively rapid compared to thermal equilibration (i.e. $t_1 << t_3$).

2.4. Perturbations and eruptions

This analysis of volcanic gas composition and SO_2 flux data is focussed on the attainment of steady state heat transfer and consequent phase relations as a magmatic gas expands adiabatically through fracture arrays from lithostatic pressure to the surface. Volcano history is predominantly quiescent with ongoing discharge of a magmatic gas plume or lower power diffuse degassing through the vent and flanks, sometimes with low discharge 'magmatic gas chimneys' recognized locally in summit areas (Giggenbach, 1990; Reyes et al., 1993). Quiescent or steady state periods are interrupted irregularly by eruptive episodes of very short to long term duration. The most dangerous events, such as Pinatubo (1991) and Nabro volcano (2011), are those with several hundred years of latency. Figure 3 compares the estimated thermal flux of quiescent stage, continuously degassing volcanic systems (Table 3) with those obtained from the eruptive yields of SO_2 for eruptions of several volcanic systems. Conversion to total gas yield through equation 3 provides an estimate of the power in MW_H of each eruption, which at $10^{2.8\text{-}7.33}$ MW_H are several orders of magnitude higher than the quiescent continuously degassing states ($10^{52\text{-}5.5}$ MW_H). These estimates of the thermal transport due to gas expansion compare well with total thermal power estimates ($10^{4.0\text{-}9.0}$ MW_H) based on the erupted mass of volcanic material for basaltic fissure to Plinean eruptions (Pyle, 2015).

Transient or peak SO_2 discharges are commonly ascribed to magma movements in shallow complex sub-volcanic 'chambers', but data for sustained quiescent stage volcanic gas plumes are likely to relate to the steady release of gas from a subsurface gas reservoir that is maintained by the steady flux of magmatic gas through the infrastructure of a volcanic system as illustrated in Figure 4. This schematic view highlights the single phase gas core of volcanic systems (Henley and Ellis, 1983; Henley and McNabb, 1978) and gas release through the surface as a gas plume, as fumaroles and solfatara and more diffusely through the flanks of the volcanic superstructure (Delmelle et al., 2015). Temporal changes in gas pressure in the gas core may relate to high level intrusive activity and seismicity and translate into observable changes in the monitored SO_2 flux at surface (Fischer et al., 1997) that may be associated with local phreatic eruptions.

The relative thermal powers of quiescent volcanic systems approximated here from SO_2 flux data are to be regarded as minima since subsurface heat and SO_2 losses occur through dispersion into geothermal regimes around the expanding gas core and condensation into high level aquifers (Symonds et al., 2001) and to a minor extent through sulfate forming reactions along fractures (Henley et al., 2015). For erupting volcanoes SO_2 losses may be regarded as negligible as they release gas from the pressurised core of the system and directly from high level intrusives. However the higher power and consequent larger component of water and particulates in the eruption column then reduces the effectiveness of remote sensing methods for SO_2 flux.

For monitoring purposes fluctuations of the characteristic temporal pattern of the observed SO_2 flux of a volcano are clearly best utilised directly for ongoing hazard assessment. At Stromboli SO_2 flux

may vary over periods of a few months from an oscillating base line of about 100 tonnes per day to shorter periods of over 800 tonnes per day (Burton et al., 2009). Hidalgo et al. (2015) record similar temporal variation for the Tungurahua volcano, Ecuador.

Relatively small and rapid temporal variations in forcing might be expected to have minimal effect on the gas expansion process. The heat capacity of the thermal buffer of the host rock will tend to smooth fluctuations towards the underlying mean state by exchanging heat with the gas on these relatively short timescales. An eruption, however, corresponds to a large amplitude perturbation, and we suggest a further timescale t_r of relevance – namely that required in the quiescent degassing state (in which the system spends most of its time) to replenish the gas volume (equal to $\phi A_s h$) held in the host rock. If M is the rate of mass release and ρ_w a representative density for the source gas, respectively,

$$t_r \sim \frac{\phi A_s h}{M/\rho_w}. \qquad (10)$$

Estimating M from surface observations for the range of quiescent stage, continuously degassing volcanic systems (Table 1) and taking ρ_w to be 150 kg/m^3 gives values for t_r ranging from order one month to more than 20 years, the limits corresponding to the most and least active volcanic systems, respectively. The majority of volcanic systems are characterised by values of t_r and t_3 of the same order of magnitude.

The time scales estimated here to attain a steady thermal state are commensurate with those observed during volcanic cycles from quiescent toward eruptive and emphasize the importance of source strength and the characteristic dimensions of the fracture array through which gas expands toward the surface. The latter is then a characteristic dimension for a given volcano that strongly influences the cyclicity of discharge and is observed through a variety of surface phenomena often relating to changes in local hydrology (Newhall et al., 2002) and affecting hot springs, solfatara and volcanic lakes.

Rapid changes in source strength due to intrusion activity and gas release (Blundy et al., 2010) lead to magmatic vapor plume expansion and eventual breakout through the surface, potentially triggering and sustaining a Plinean eruption[5]. At Pinatubo, for example, precursor events including steam explosions consequent on increased heat flow, continued for a period of 11 weeks prior to the immense 1991 eruption and SO_2 flux also increased progressively, reaching 0.013 megatonnes per day immediately before the Plinean event. The Plinean eruption itself released about 20 megatonnes of SO_2 (Bluth et al., 1992; Daag et al., 1996), a mass far larger than appears reasonable for storage in a reasonably scaled intrusion (Newhall et al., 2002). Models based on gas exsolution from reasonable sized intrusions therefore appear untenable. The total gas phase released, with inclusion of water, is about 60 megatonnes based on the reference arc gas composition. At 1000 bars pressure this mass of gas equates to the volume of a cylinder of depth 8km and radius about 8km, and requires a storage volume ten times larger if the average porosity was about ten percent. An eruption of this scale therefore requires mining of a pressurised gas reservoir to mid-crustal depth and poses some new questions about how Plinean scale eruptions achieve this. One possibility

[5] For completeness we note that eruptive phenomena themselves occur through more complex irreversible expansion processes involving heat exchange with a high density of particulate material in the gas phase.

is that increased source strength first builds pressure inside the superstructure of the volcano but that the pressure increase is limited to the tensile strength of the rock material; 5 to 50 bars. Fracturing ensues to initiate an ongoing series of fracturing events through to initial break out at the surface which then removes a small proportion of rock mass. An immediate positive feedback ensues due to lithostatic load removal, feeding back on itself through further rock failure and rock removal into the developing ash plume as it rapidly extends deeper and deeper into the gas pressured reservoir. This proceeds to feed on itself until the gas reservoir is exhausted. Although speculative, this is potentially a useful starting point for discussion of Plinean eruption mechanisms and hazard assessment, with a focus on the gas phase that is progressively stored inside volcanic systems and fed from evolving intrusion complexes.

3.0 Summary

Volcanic systems are complex and their behaviour embraces a range of interactive processes including deep and shallow intrusions, gas exsolution from magmas, gas mixture expansion through fractured rock and interactions with surrounding deep and shallow groundwater systems (Henley and Berger, 2013; Henley and McNabb, 1978). Here we have focussed on the thermal power of volcanic systems in their quiescent through eruptive cycles by considering the scale of heat transfer between expanding magmatic gas mixtures and the fractured rocks through which they pass. SO_2 flux data, now increasingly available for active volcanoes, provides the basis from which to estimate total heat and mass transfer through to the surface. For quiescent, continuously degassing volcanoes mass transfer ranges between about 1500 and 500,000 tonnes per day with equivalent heat transfer of about 10^2 to $10^{4.4}$ MW_H. In eruptive cycles these mass transfers increase by more than 2 orders of magnitude with Plinean eruptions such as Pinatubo in 1991 , a further one or two orders of magnitude larger, a scale demanding consideration of stored pressurised gas as the prime driver of catastrophic eruptions.

Consideration of heat and mass flux in volcanic systems also underpins quantification of the scale of heat transfer to fractured rock mass as magmatic gas expands to the surface and the time scale over which gas expansion may be modelled as adiabatic. In turn this enables modelling of pressure-temperature changes experienced by volcanic gas inside the superstructure of volcanoes, the phase changes occurring during expansion and consequent changes in gas phase chemistry in fumaroles relative to magmatic source conditions. The approach to these is necessarily general but provides a useful basis from which to consider and track the unique behaviour of individual volcanoes and make comparisons between volcanic systems.

Acknowledgements

We wish to acknowledge the major contribution to establishing the foundations of modern volcanology by Jean Verhoogen (1912-1993). *The thermodynamics of a magmatic gas phase* (Verhoogen, 1949) was the first modern attempt to provide a foundation through which to systematically explore the behaviour of magmatic gases and their crucial role in driving the behaviour of volcanoes. Sampling and analysis of volcanic gases was then in its infancy (Jaggar, 1940), access being a major and continuing issue. Recognising this, Verhoogen (1939) became a

pioneer of remote sensing of volcanic gas emissions at Nyamligara in the now Democratic Republic of the Congo, a volcano that is now known to be one of the most powerful volcanic sources of volcanic SO_2 on Earth. Graton (1945) must also be acknowledged for the insights into volcanic heat transfer that triggered a lively discussion with Verhoogen (1946). We also acknowledge the spectacular advances made by so many in the careful and often dangerous sampling of volcanic gas discharges and the development of the powerful modern technology for SO_2 discharge monitoring that here underpins our attempt to quantify the power of active volcanoes.

We thank Penny King and Chris Renggli for constructive comment and enthusiasm in unravelling the behaviour of gases inside volcanoes. RWH was partially supported by Australian Research Council funding (DP150104604). Constructive review comments from Maarten de Moor were much appreciated.

References

Berger, B.R., Henley, R.W., Lowers, H.A. and Pribil, M.J., 2014. The Lepanto Cu–Au deposit, Philippines: A fossil hyperacidic volcanic lake complex. Journal of Volcanology and Geothermal Research, 271: 70-82.

Blundy, J., Cashman, K.V., Rust, A. and Witham, F., 2010. A case for CO 2-rich arc magmas. Earth and Planetary Science Letters, 290(3): 289-301.

Bluth, G.J., Doiron, S.D., Schnetzler, C.C., Krueger, A.J. and Walter, L.S., 1992. Global tracking of the S02 clouds from the June, 1991 Mount Pinatubo eruptions. Geophys. Res. Lett, 19(2): 151-154.

Bonafede, M. and Mazzanti, M., 1997. Hot fluid migration in compressible saturated porous media. Geophysical Journal International, 128(2): 383-398.

Botcharnikov, R.E., Shmulovich, K.I., Tkachenko, S.I., Korzhinsky, M.A. and Rybin, A.V., 2003. Hydrogen isotope geochemistry and heat balance of a fumarolic system: Kudriavy volcano, Kuriles. Journal of volcanology and geothermal research, 124(1): 45-66.

Burton, M., Caltabiano, T., Murè, F., Salerno, G. and Randazzo, D., 2009. SO 2 flux from Stromboli during the 2007 eruption: Results from the FLAME network and traverse measurements. Journal of Volcanology and Geothermal Research, 182(3): 214-220.

Carmichael, I.S., Turner, F.J. and Verhoogen, J., 1974. Igneous petrology. McGraw-Hill.

Collinson, A. and Neuberg, J., 2012. Gas storage, transport and pressure changes in an evolving permeable volcanic edifice. Journal of Volcanology and Geothermal Research, 243: 1-13.

Daag, A., Tubianosa, B., Newhall, C., Tungol, N., Javier, D., Dolan, M., Delos Reyes, P., Arboleda, R., Martinez, M. and Regalado, T., 1996. Monitoring sulfur dioxide emission at Mount Pinatubo. Fire and Mud: eruptions and lahars of Mount Pinatubo, Philippines: 409-414.

de Moor, J.M., Fischer, T.P., Sharp, Z.D., King, P.L., Wilke, M., Botcharnikov, R.E., Cottrell, E., Zelenski, M., Marty, B., Klimm, K., Rivard, C., Ayalew, D., Ramirez, C. and Kelley, K.A., 2013. Sulfur degassing at Erta Ale (Ethiopia) and Masaya (Nicaragua) volcanoes: Implications for degassing processes and oxygen fugacities of basaltic systems. Geochemistry, Geophysics, Geosystems, 14(10): 4076-4108.

Delmelle, P., Henley, R.W., Opfergelt, S. and Detienne, M., 2015. Summit acid crater lakes and flank instability in composite volcanoes, Volcanic Lakes. Springer, pp. 289-305.

Elder, J.W., 1965. Physical processes in geothermal areas. Terrestrial heat flow: 211-239.

Fischer, T.P., 2008. Fluxes of volatiles (H2O, CO2, N2, Cl, F) from arc volcanoes. Geochemical Journal, 42(1): 21-38.

Fischer, T.P., Garzon, G., Gómez, D., Narváez, L., Ordón, M., Ortega, A., Stix, J., Torres, R. and Williams, S.N., 1997. SO 2 fluxes from Galeras Volcano, Colombia, 1989–1995: Progressive degassing and conduit obstruction of a Decade Volcano. Journal of Volcanology and geothermal research, 77(1): 195-208.

Fisher, R., 1964. Geothermal heat flow at Wairakei during 1958. New Zealand Journal of Geology and Geophysics, 7(1): 172-184.

Giggenbach, W., 1987. Redox processes governing the chemistry of fumarolic gas discharges from White Island, New Zealand. Applied Geochemistry, 2(2): 143-161.

Giggenbach, W., 1990. The chemistry of fumarolic vapor and thermal-spring discharges from the Nevado del Ruiz volcanic-magmatic-hydrothermal system, Colombia. Journal of Volcanology and Geothermal Research, 42(1): 13-39.

Giggenbach, W., 1996. Chemical composition of volcanic gases, Monitoring and mitigation of volcano hazards. Springer, pp. 221-256.

Giggenbach, W. and Matsuo, S., 1991. Evaluation of results from Second and Third IAVCEI field workshops on volcanic gases, Mt Usu, Japan, and White Island, New Zealand. Applied Geochemistry, 6(2): 125-141.

Giggenbach, W. and Sheppard, D., 1989. Variations in the temperature and chemistry of White Island fumarole discharges 1972–85. NZ Geol. Surv. Bull, 103(119.126).

Giggenbach, W., Tedesco, D., Sulistiyo, Y., Caprai, A., Cioni, R., Favara, R., Fischer, T., Hirabayashi, J.-I., Korzhinsky, M. and Martini, M., 2001. Evaluation of results from the fourth and fifth IAVCEI field workshops on volcanic gases, Vulcano island, Italy and Java, Indonesia. Journal of Volcanology and Geothermal Research, 108(1): 157-172.

Graton, L., 1945. Conjectures regarding volcanic heat. Am. J. Sci, 243: 135-259.

Hautmann, S., Witham, F., Christopher, T., Cole, P., Linde, A.T., Sacks, I.S. and Sparks, R.S.J., 2014. Strain field analysis on Montserrat (WI) as tool for assessing permeable flow paths in the magmatic system of Soufrière Hills Volcano. Geochemistry, Geophysics, Geosystems, 15(3): 676-690.

Heap, M., Farquharson, J., Baud, P., Lavallée, Y. and Reuschlé, T., 2015. Fracture and compaction of andesite in a volcanic edifice. Bulletin of Volcanology, 77(6): 1-19.

Henley, R. and Hughes, G., 2000. Underground fumaroles:" Excess heat" effects in vein formation. Economic Geology, 95(3): 453-466.

Henley, R.W. and Berger, B.R., 2013. Nature's refineries — Metals and metalloids in arc volcanoes. Earth-Science Reviews, 125: 146-170.

Henley, R.W. and Ellis, A.J., 1983. Geothermal systems ancient and modern: a geochemical review. Earth-Science Reviews, 19(1): 1-50.

Henley, R.W., King, P.L., Wykes, J.L., Renggli, C.J., Brink, F.J., Clark, D.A. and Troitzsch, U., 2015. Porphyry copper deposit formation by sub-volcanic sulphur dioxide flux and chemisorption. Nature Geoscience, 8(3): 210-215.

Henley, R.W. and McNabb, A., 1978. Magmatic vapor plumes and ground-water interaction in porphyry copper emplacement. Economic Geology, 73(1): 1-20.

Hidalgo, S., Battaglia, J., Arellano, S., Steele, A., Bernard, B., Bourquin, J., Galle, B., Arrais, S. and Vásconez, F., 2015. SO 2 degassing at Tungurahua volcano (Ecuador) between 2007 and 2013: Transition from continuous to episodic activity. Journal of Volcanology and Geothermal Research, 298: 1-14.

Hurwitz, S., Kipp, K.L., Ingebritsen, S.E. and Reid, M.E., 2003. Groundwater flow, heat transport, and water table position within volcanic edifices: implications for volcanic processes in the Cascade Range. Journal of Geophysical Research: Solid Earth (1978–2012), 108(B12).

Jaggar, T.A., 1940. Magmatic gases. American Journal of Science, 238(5): 313-353.

La Felice, S., Montanari, D., Battaglia, S., Bertini, G. and Gianelli, G., 2014. Fracture permeability and water–rock interaction in a shallow volcanic groundwater reservoir and the concern of its interaction with the deep geothermal reservoir of Mt. Amiata, Italy. Journal of Volcanology and Geothermal Research, 284: 95-105.

Massiot, C., McNamara, D.D., Nicol, A., Archibald, G. and Townend, J., 2014. Fracture geometries and processes in andesites at Mt Ruapehu, New Zealand: implications for the fracture modelling of the Rotokawa Geothermal Field.

Mather, T., Pyle, D., Tsanev, V., McGonigle, A., Oppenheimer, C. and Allen, A., 2006. A reassessment of current volcanic emissions from the Central American arc with specific examples from Nicaragua. Journal of volcanology and geothermal Research, 149(3): 297-311.

Matsushima, N., Kazahaya, K., Saito, G. and Shinohara, H., 2003. Mass and heat flux of volcanic gas discharging from the summit crater of Iwodake volcano, Satsuma-Iwojima, Japan, during 1996–1999. Journal of volcanology and geothermal research, 126(3): 285-301.

McCormick, B.T., Edmonds, M., Mather, T.A., Campion, R., Hayer, C.S., Thomas, H.E. and Carn, S.A., 2013. Volcano monitoring applications of the Ozone Monitoring Instrument. Geological Society, London, Special Publications, 380(1): 259-291.

Melnikov, D. and Ushakov, S., 2011. SO2 GAS EMISSION OF MUTNOVSKY AND GORELY VOLCANOES (KAMCHATKA): SATELLITE DATA AND GROUND-BASED OBSERVATIONS, Abstract CCVG11 Workshop on Volcanic Gases. Kamchatka, Russia, pp. 33.

Mizutani, Y. and Sugiura, T., 1982. Variations in chemical and isotopic compositions of fumarolic gases from Showashinzan volcano, Hokkaido, Japan. Geochemical Journal, 16(2): 63-71.

Mori, T., Shinohara, H., Kazahaya, K., Hirabayashi, J.i., Matsushima, T., Mori, T., Ohwada, M., Odai, M., Iino, H. and Miyashita, M., 2013. Time - averaged SO2 fluxes of subduction - zone volcanoes: Example of a 32 - year exhaustive survey for Japanese volcanoes. Journal of Geophysical Research: Atmospheres, 118(15): 8662-8674.

Newhall, C., Power, J. and Punongbayan, R., 2002. To make grow. Science, 295(5558): 1241-1242.

Pyle, D.M., 2015. Sizes of volcanic eruptions. In: H. Sigurdsson (Editor), The Encyclopedia of Volcanoes. Academic Press, London.

Reyes, A.G., Giggenbach, W.F., Saleras, J.R., Salonga, N.D. and Vergara, M.C., 1993. Petrology and geochemistry of Alto Peak, a vapor-cored hydrothermal system, Leyte Province, Philippines. Geothermics, 22(5): 479-519.

Sano, Y. and Fischer, T.P., 2013. The analysis and interpretation of noble gases in modern hydrothermal systems, The Noble Gases as Geochemical Tracers. Springer, pp. 249-317.

Shinohara, H., 2008. Excess degassing from volcanoes and its role on eruptive and intrusive activity. Reviews of Geophysics, 46(4).

Shinohara, H., 2013. Volatile flux from subduction zone volcanoes: Insights from a detailed evaluation of the fluxes from volcanoes in Japan. Journal of Volcanology and Geothermal Research, 268: 46-63.

Symonds, R., Gerlach, T. and Reed, M., 2001. Magmatic gas scrubbing: implications for volcano monitoring. Journal of Volcanology and Geothermal Research, 108(1): 303-341.

Symonds, R.B., Rose, W.I., Bluth, G.J. and Gerlach, T.M., 1994. Volcanic-gas studies; methods, results, and applications. Reviews in Mineralogy and Geochemistry, 30(1): 1-66.

Tibaldi, A., 2015. Structure of volcano plumbing systems: A review of multi-parametric effects. Journal of Volcanology and Geothermal Research, 298: 85-135.

Verhoogen, J., 1946. Volcanic heat. American Journal of Science, 244(11): 745-771.

Verhoogen, J., 1949. Thermodynamics of a magmatic gas phase. University of California Publications, Berkeley, CA.

Williams, H. and McBirney, A., 1979. Volcanology, 397 pp. Free man, Cooper & Co., San Francisco.

Zelenski, M. and Taran, Y., 2011. Geochemistry of volcanic and hydrothermal gases of Mutnovsky volcano, Kamchatka: evidence for mantle, slab and atmosphere contributions to fluids of a typical arc volcano. Bulletin of volcanology, 73(4): 373-394.

Figure Captions

Figure 1. Elements of the fractured block model showing the relationship between magmatic gas flux and the fractured rock matrix blocks of a volcano due to conduction (inset) to evolve thermal boundary layers in the blocks. Predicted timescales $t_{3'}$ for quasi-adiabatic behaviour (discrete points) and t3'' for fully adiabatic behaviour (solid lines) as a function of the power, E, of measured quiescent volcanic systems (see Table 1). Data for fracture spacings in the host rock of 1, 10 and 50 m are shown for temperature perturbations of 50, 250 and 500 °C. Note that the time scale curve for d = 10m and ΔT=50°C is coincident with that of d=50m and ΔT = 250°C. Also plotted is the replenishment timescale, t_r, as discussed in the text. For reference the broad range of time scales and power for eruptive and quiescent volcanic discharges are also shown as discussed in the text (Figure 3 and Supplement 1).

Figure 2. Equilibrium composition of the median arc and mantle-related volcanic gas mixtures (Table 1) as a function of temperature at 1 bar total pressure. Note the low concentrations of minor sulfur species in relation to H_2S and SO_2 and the very rapid decrease of the H_2S:SO_2 ratio above 800 °C. Elemental sulfur as a liquid phase has not been included because, like H_2S, there is no evidence that SO_2 reduction during expansion occurs at a sufficient rate to nucleate significant sulfur (Giggenbach, 1987) although it may be present in aerosols. A wide range of C-O-H-S species such as SO_3, H_2SO_4,COS and S_n gaseous species occur at much lower concentrations

Figure 3. Comparison of estimated thermal transport due to gas release during eruptive events with quiescent discharge degassing of arc and mantle-sourced volcanoes. SO_2 yield data used for the estimation of eruptive yields are primarily from McCormick et al. (2013).For comparison the natural

heat flux of the Wairakei geothermal and the electric power production of the Three Gorges Dam power stations are $10^{2.6}$ and $10^{4.4}$ respectively.

Figure 4. Schema for heat transfer due to volcanic gas from a lithostatic pressured environment to the surface showing the development of a single phase, gas-cored volcanic gas plume, heat dispersion by mixing on its margin to develop laterally extensive geothermal systems (G), and the regime of relatively shallow secondary processes related to capture and condensation of gas mixtures separated from the plume near surface (S). Dispersion on the margin coupled with loss of pressure and adiabatic temperature decrease produce a two phase (liquid plus vapor or halite plus vapor) margin. When the gas core is sufficiently powerful to break through to the surface a continuous degassing-based atmospheric plume and high temperature fumaroles are developed. Its aspect ratio may vary through time (Giggenbach and Sheppard, 1989) due to changes in source strength and permeability(Henley and Berger, 2013). Note the contributions to gas flux from high level intrusive activity. ΣH_{mg} is the heat flux as magmatic gas is throttled to quasi-hydrostatic pressure and ΣH_g is the thermal yield observed through SO_2 flux data for the volcanic system. Within the gas core regime decompression and mixing at its margin develops two phase conditions but gas phase separation occurs only near surface to form solfatara and associated relatively low temperature fumaroles.

Table Captions

Table 1. Discharge power of continuous (quiescent) degassing volcanoes estimated from SO2 flux data and the H_2O/SO_2 gas mixture ratio for median arc and mantle sourced volcanic gases and their enthalpies as described in the text. Data sources as follows: 1 = Shinohara (2008), 2 = McCormick et al. (2013), 3 = Mori et al. (2013), 4 = Mather et al. (2006), 5= Melnikov and Ushakov (2011), 6 = Hidalgo et al. (2015), 7 =Fisher (1964). Figures have not been rounded in order to preserve the calculation routine.

Table 2. Median values of major components of volcanic gas mixtures sampled from fumaroles on active arc and mantle-sourced volcanoes at temperatures > 500 °C. The full data set is provided in Supplement 2.

Table 1

Click here to download Table: Table 1 gas composition stats.docx

Setting	Volcano	Range °C	n	t °C	H_2O	CO_2	S_t	HCl	HF	H_2	mole %	Mole fraction total gas	H_2O/SO_2	CO_2/S_t	Enthalpy (1bar)
Arc	Maxima	>500 °C	66	1100	99.88	12.40	6.98	2.75	0.66	3.02		0.14	14268.6	78.3	4894
Arc	Minima	>500 °C		505	84.77	0.02	0.01	0.02	0.00	0.00		0.00	12.1	0.2	3499
Arc	Mean	>500 °C		766	94.76	2.63	1.38	0.55	0.09	0.61		0.05	674.2	5.7	4080
Arc	**Median**	**>500 °C**		**763**	**95.16**	**1.81**	**1.18**	**0.42**	**0.03**	**0.54**		**0.04**	**79.9**	**1.6**	**4074**
Arc	Mean	800 - 1000 **°C**	23	861	94.5	1.8	1.8	0.7	0.1	0.8		0.05	167.6	2.7	4305
Arc	**Median**	**800 - 1000 °C**		**870**	**95.0**	**1.6**	**1.8**	**0.5**	**0.04**	**0.8**		**0.05**	**53.7**	**0.9**	**4326**
Arc	***Median (adj.)[1]***	***800 - 1000 °C***		***870***	***95.1***	***1.75***	***1.3***	***0.5***	***0.03***	***0.8***		***0.05***	***75.8***	***0.9***	***4039***
Arc	**Median**	**> 800 °C**	**28**	**874**	**95.0**	**1.51**	**1.25**	**0.54**	**0.08**	**0.8**		**0.05**	**53.7**	**0.9**	**4050**
Mantle	Maxima		8	1131	81.13	36.40	15.90	0.81	2.37	0.75		0.398	41.4	26.0	4973
Mantle	Minima			915	57.90	3.15	1.40	0.10	0.19	0.75		0.155	5.0	0.2	4434
Mantle	Mean			1042	72.4	15.55	8.72	0.51	0.52	0.75		0.251	13.9	5.2	4746
Mantle	**Median**			**1092**	**79.29**	**9.90**	**7.80**	**0.65**	**0.32**	**0.75**		**0.19**	**12.3**	**1.8**	**4853**

[1] Median excluding high outlier HCl concentrations from Etna and Vulcano analyses.

Table 2

Click here to download Table: Table 2.flux.docx

Volcano	Provenance	SO_2 t/day	H_2O t/day	E kJ/sec	log MW_H	Source
Kilauea	*Mantle*	*800*	*2,295*	*128,908*	*2.1*	1
Etna	Arc	21,000	447,694	22,415,777	4.4	2
Etna	Arc	4,000	85,275	4,269,672	3.6	1
Bagana	Arc	3,300	70,352	3,522,479	3.5	1
Lascar	Arc	2,400	51,165	2,561,803	3.4	1
Miyakejima	Arc	2,119	45,174	2,261,859	3.4	3
Pacaya	Arc	2,000	42,638	2,134,836	3.3	4
Ruiz	Arc	1,900	40,506	2,028,094	3.3	1
Sakurajima	Arc	1,641	34,984	1,751,633	3.2	3
Manam	Arc	920	19,613	982,025	3.0	1
Yasur	Arc	900	19,187	960,676	3.0	1
Masaya	Arc	790	16,842	843,260	2.9	4
Stromboli	Arc	730	15,563	779,215	2.9	1
Langila	Arc	690	14,710	736,518	2.9	1
Galeras	Arc	650	13,857	693,822	2.8	1
Fuego	Arc	640	13,644	683,148	2.8	4
San Cristobal	Arc	590	12,578	629,777	2.8	4
Satsuma-Iwojima	Arc	570	12,152	608,428	2.8	1
Wairakei Geothermal System					2.6	7
Mutnovsky	Arc	330	7,035	352,248	2.5	5
Arenal	Arc	180	3,837	192,135	2.3	4
Tungurahua volcano	Arc	1,424	30,358	1,520,003	3.2	6
Tungurahua volcano	Arc	735	15,669	784,552	2.9	6
Tungurahua volcano	Arc	73	1,556	77,922	1.9	6

Figure 1

Click here to download high resolution image

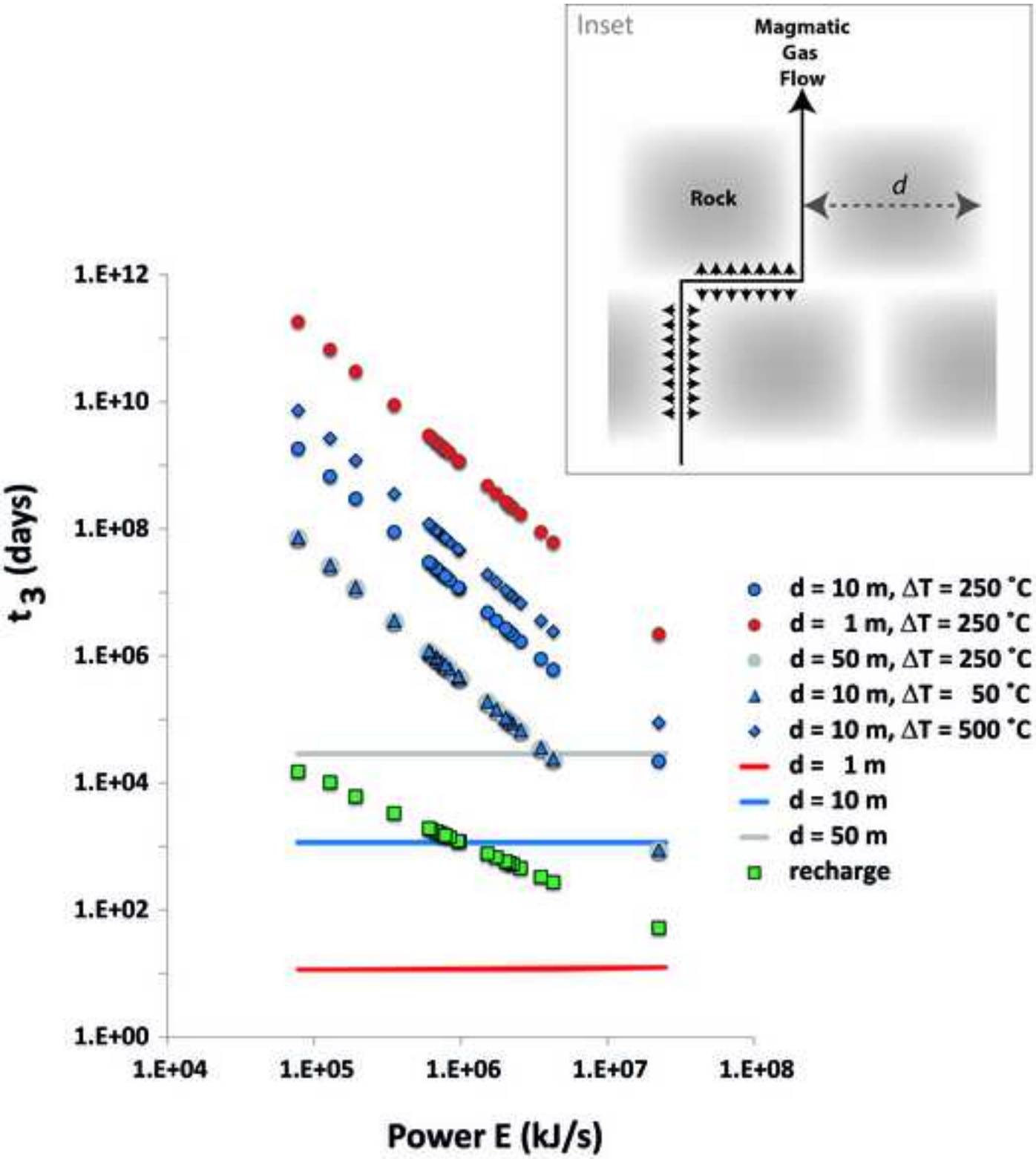

Figure 2

Click here to download high resolution image

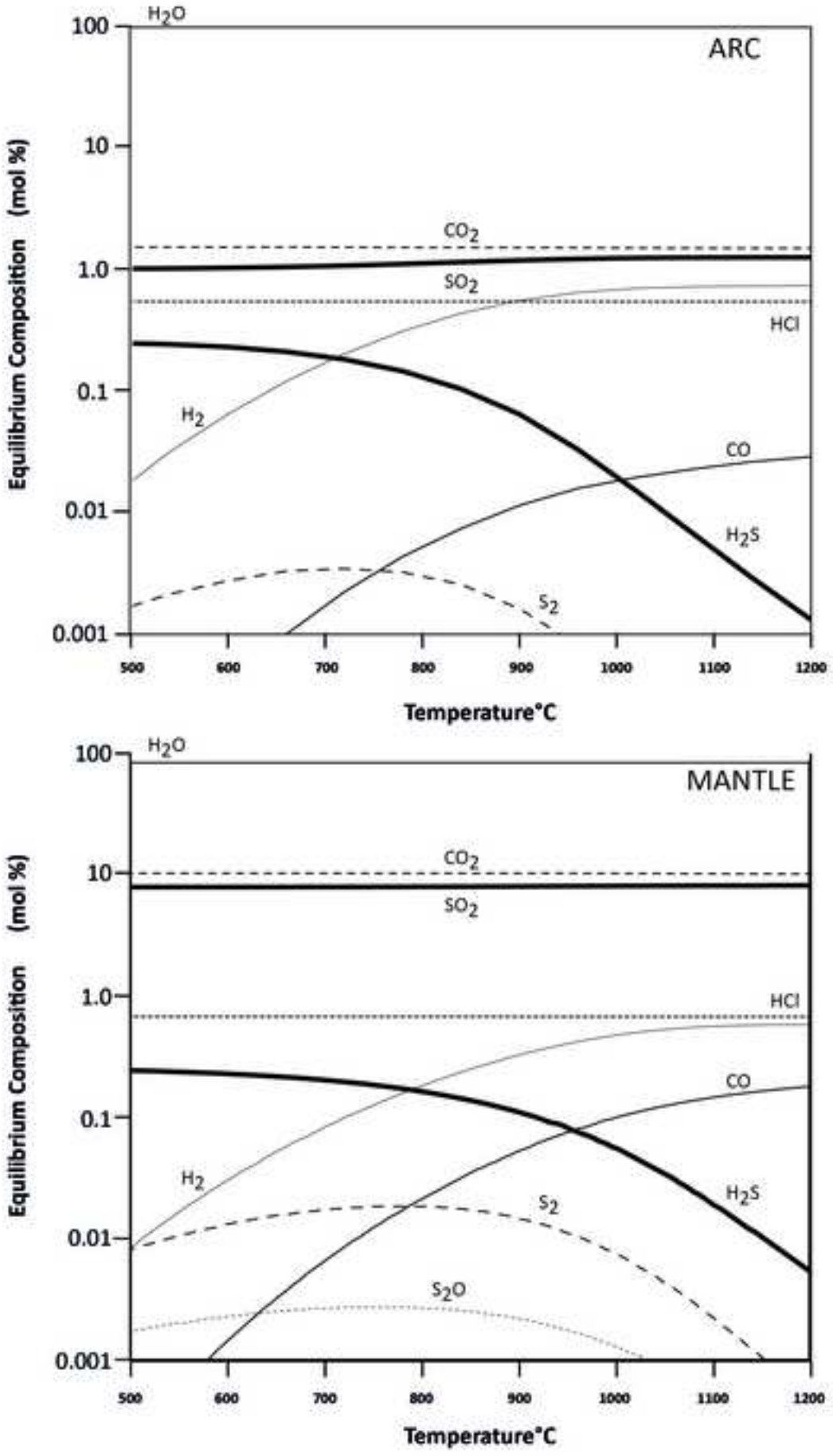

Figure 3

Click here to download high resolution image

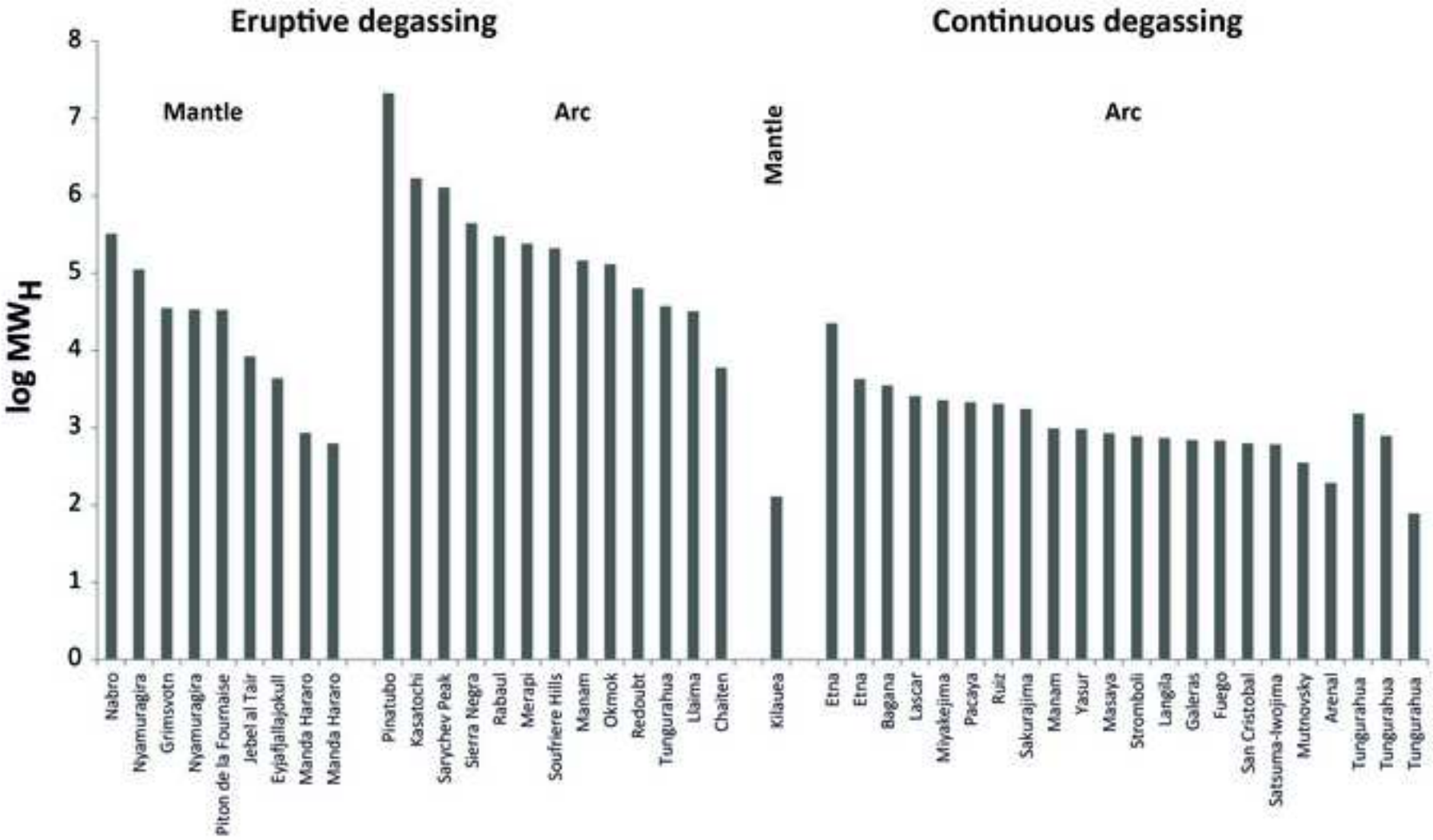

Figure 4

Click here to download high resolution image

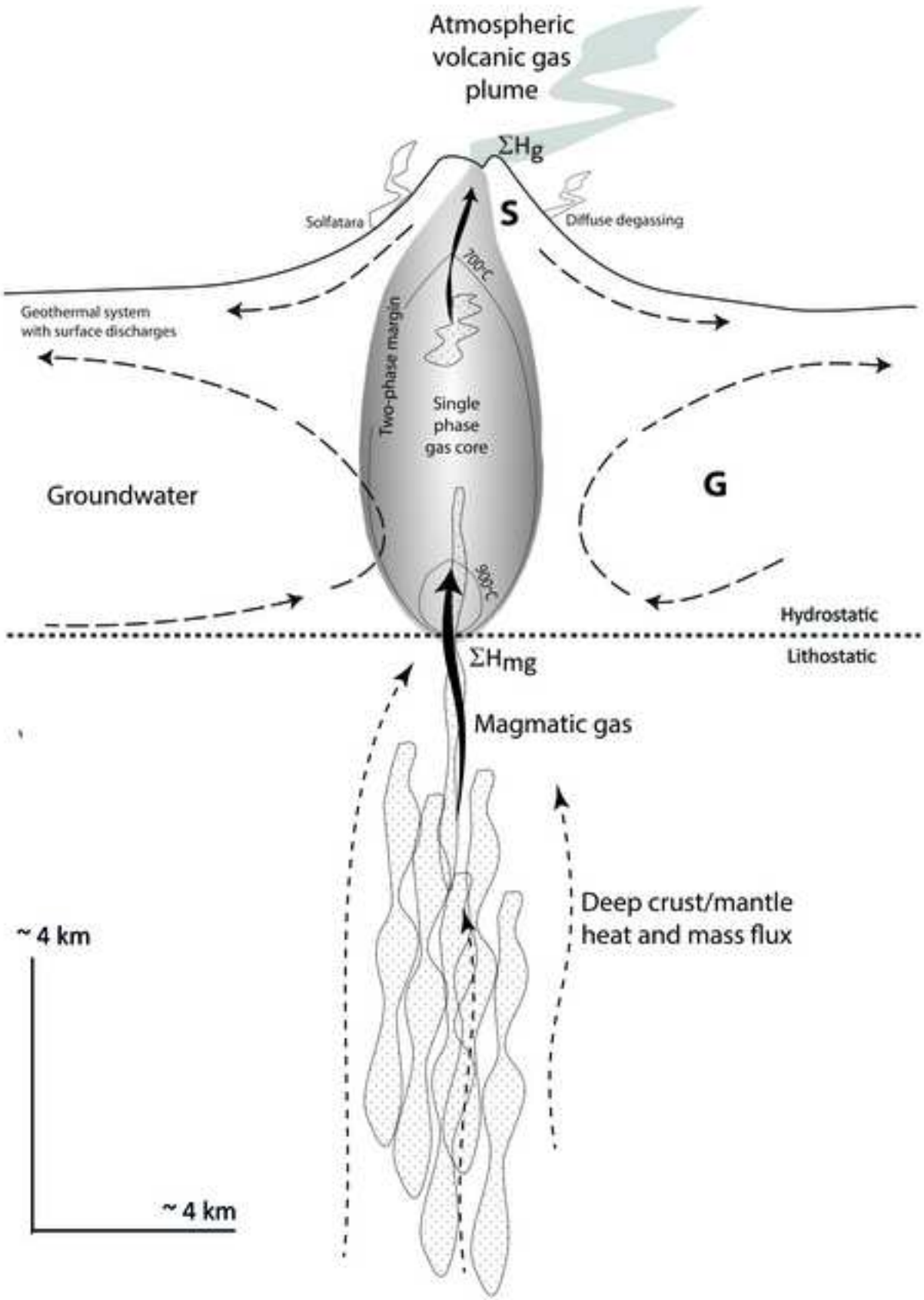

Electronic Supplementary Material 1 (online publication only)

Click here to download Electronic Supplementary Material (online publication only): Supplement Tables 1 and 2.pdf